Cell

Opposing Wnt Pathways Orient Cell Polarity during Organogenesis

Jennifer L. Green,[1] Takao Inoue,[1] and Paul W. Sternberg[1,*]
[1]Howard Hughes Medical Institute/Division of Biology, California Institute of Technology, Mail Code 156-29, Pasadena, CA 91125, USA
*Correspondence: pws@caltech.edu
DOI 10.1016/j.cell.2008.06.026

SUMMARY

The orientation of asymmetric cell division contributes to the organization of cells within a tissue or organ. For example, mirror-image symmetry of the *C. elegans* vulva is achieved by the opposite division orientation of the vulval precursor cells (VPCs) flanking the axis of symmetry. We characterized the molecular mechanisms contributing to this division pattern. Wnts MOM-2 and LIN-44 are expressed at the axis of symmetry and orient the VPCs toward the center. These Wnts act via Fz/LIN-17 and Ryk/LIN-18, which control β-catenin localization and activate gene transcription. In addition, VPCs on both sides of the axis of symmetry possess a uniform underlying "ground" polarity, established by the instructive activity of Wnt/EGL-20. EGL-20 establishes ground polarity via a novel type of signaling involving the Ror receptor tyrosine kinase CAM-1 and the planar cell polarity component Van Gogh/VANG-1. Thus, tissue polarity is determined by the integration of multiple Wnt pathways.

INTRODUCTION

In organized epithelial tissues, the polarity of component cells is precisely controlled, and its loss is a major factor in tumor formation and progression (reviewed by Wodarz and Nathke, 2007). During development, the coordination of cell polarity is requisite for normal tissue architecture. For example, the orientation of an asymmetrically dividing cell will determine the arrangement of the daughter cells within the tissue. This is particularly important during organogenesis, where oriented divisions contribute greatly to organ size and shape (Baena-Lopez et al., 2005; Strutt, 2005), and cells often adopt a novel coordinate system to suit the architectural needs of the developing organ. In such cases, cells in an organ primordium must interpret complex and sometimes conflicting polarizing information. A simple model for the study of this phenomenon is *C. elegans* vulval development, in which certain cells within the same epithelium invariantly divide in opposite orientations. Here, we investigate how multiple Wnt signals interact to orient the vulval precursor cells (VPCs).

Wnts are a class of secreted glycoproteins that are conserved among all metazoa. Work from several systems reveals a variety of mechanisms by which Wnt signals are transduced (reviewed by Gordon and Nusse, 2006). In one well-conserved pathway, Wnt binding to Frizzled receptors leads to activation of target genes through the TCF/β-catenin transcription factor complex. However, β-catenin-independent Wnt pathways also exist. The planar cell polarity (PCP) pathway is mediated by Frizzled but involves components different from the pathway leading to TCF/β-catenin regulation. More recently, receptor tyrosine kinases (RTKs) Ryk and Ror have emerged as alternative Wnt-binding receptors, although function of these RTK Wnt receptors is not yet well understood.

The *C. elegans* vulva is formed from the reproducible divisions of three VPCs—P5.p, P6.p, and P7.p—arranged along the anterior-posterior (AP) axis in the ventral epithelium (Figure 1) (reviewed by Sternberg, 2005; Sulston and Horvitz, 1977). The Wnt, EGF, and Notch signaling pathways instruct the VPCs to adopt fates that correspond to particular lineage patterns. P6.p, the central VPC, divides symmetrically three times to produce eight cells that detach from the epidermis and form the vulval lumen (the 1° lineage pattern). P5.p and P7.p, after three rounds of asymmetric cell division (the 2° lineage pattern), produce the anterior and posterior sides of the vulva. The outermost progeny of both 2° VPCs adhere to the epidermis, whereas the inner 2° progeny detach from the epidermis and join the 1° progeny cells to form the lumen. The 2° progeny are arranged so that P5.p descendants display mirror-image symmetry to P7.p descendents. Thus, the vulva is organized along a proximal-distal (PD) axis with the axis of symmetry at the center. Although vulva development is one of the simplest and best understood models of organogenesis, why P5.p and P7.p divide in opposite orientations is poorly understood.

There are five Wnts in *C. elegans*: LIN-44, CWN-1, CWN-2, EGL-20, and MOM-2. LIN-44, CWN-1, CWN-2, and MOM-2 are known to regulate P7.p orientation. LIN-44 and MOM-2 play a major role and function in parallel, undefined pathways with their respective receptors, Frizzled (Fz)/LIN-17 and Ryk/LIN-18 (Ferguson et al., 1987; Gleason et al., 2006; Inoue et al., 2004; Sawa et al., 1996; Sternberg and Horvitz, 1988). In the absence of this signaling, the P7.p lineage displays the reverse, P5.p-like, orientation, such that the invaginating cells are posterior to the adherent cells (hereby called "facing posteriorly"). This reversal in the P7.p lineage results in a second invagination posterior to the main vulva, a phenotype called P-Rvl for "*p*osterior-*r*eversed *v*ulval *l*ineage," also known as Bivulva (Figure 2B) (Ferguson and Horvitz, 1985; Ferguson et al., 1987). A similar phenotype in P5.p, A-Rvl (anterior-reversed

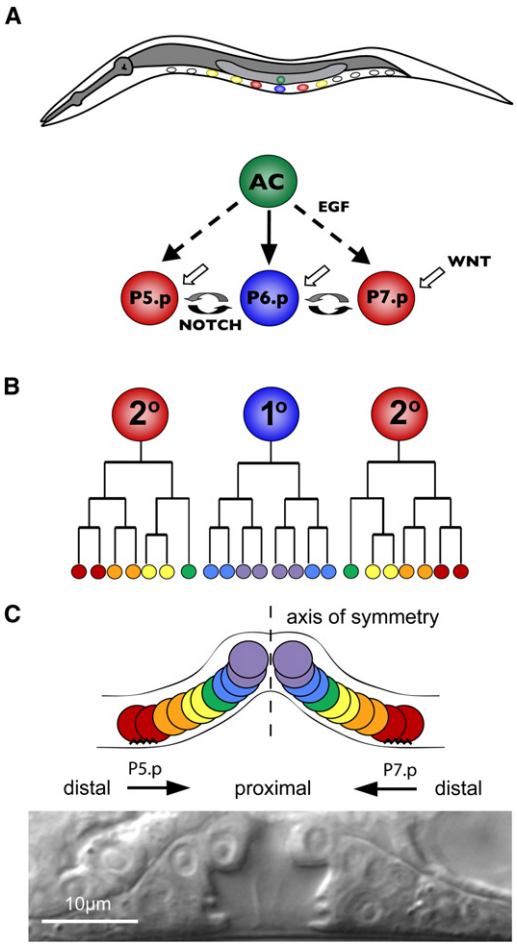

Figure 1. *C. elegans* Vulva Development

(A) Schematic of vulval induction. Anterior, left; dorsal, up.

(B) Lineage trees of the VPC progeny. P5.p, left; P6.p, center; P7.p, right.

(C) Schematic arrangement (top) of the 1° and 2° vulval lineages along a proximal-distal axis. The cells located anterior or posterior to the axis of symmetry (dashed line) display opposite orientations. The jagged lines represent adherence to the cuticle. At the bottom is a Nomarski image of a wild-type vulva at the L4 stage.

*v*ulval *l*ineage), has not been described (Figure 2C). To explain why *lin-17* and *lin-18* mutations do not affect P5.p, Deshpande et al. (2005) proposed that both P5.p and P7.p face posteriorly by default and that *lin-17* and *lin-18* reorient P7.p toward the center. However, they did not determine why the default orientation of P7.p is to face posteriorly, nor were they able to examine the role of Fz/LIN-17 and Ryk/LIN-18 in P5.p orientation.

Here, we present evidence that the Wnt signaling-independent orientation of both P5.p and P7.p is random. Wnt/EGL-20 acts as a directional cue to confer an underlying AP polarity, causing both P5.p and P7.p to face the posterior. A novel pathway involving the Ror receptor tyrosine kinase CAM-1 and the planar cell polarity component Van Gogh/VANG-1 mediates the EGL-20 signal. In response to MOM-2 and LIN-44, the central-orienting Wnts, Fz/LIN-17 and Ryk/LIN-18 instruct P5.p and P7.p to face the center, thus reversing P7.p orientation and reinforcing P5.p orientation. These results demonstrate that multiple Wnt pathways operating in different directions contribute to organized polarity in a developing organ.

RESULTS

Wnt/egl-20 Antagonizes *Fz/lin-17* and *Ryk/lin-18* in P7.p

We wished to understand the apparent default posterior-facing orientation of P5.p and P7.p. and reasoned that mutations disrupting this default polarity should suppress the P-Rvl phenotype of *lin-17* and *lin-18* mutants. As reported by Gleason et al. (2006), we found that a loss-of-function (lf) mutation in *Wnt/cwn-1* mildly suppressed the *Fz/lin-17(lf)* P-Rvl phenotype but did not significantly suppress the *Ryk/lin-18(lf)* P-Rvl phenotype (Table 1). In addition, we tested the involvement of *Wnt/egl-20*, whose role in VPC orientation was unknown and found that strong reduction-of-function (rf) and lf alleles of *Wnt/egl-20* strongly suppressed the P-Rvl phenotype of both *lin-17(lf)* and *lin-18(lf)* mutants. Thus, like *cwn-1*, *egl-20* antagonizes the function of *lin-17*, but it additionally antagonizes the function of *lin-18*. We constructed triple mutants defective in both receptors and each of these Wnts and found that mutations in *egl-20* suppressed the phenotype of *lin-17(lf); lin-18(lf)* double mutants from 100% P-Rvl to 50% P-Rvl, whereas only weak suppression was seen with *cwn-1(lf)*. Since Fz/LIN-17 and Ryk/LIN-18 function in parallel pathways to orient P7.p (Inoue et al., 2004), the ability of *egl-20* mutations to suppress the receptor double loss-of-function mutants suggests that Wnt/EGL-20 functions via a different receptor in a third parallel pathway. Moreover, EGL-20 has an opposing effect on P7.p orientation and instructs P7.p to face posteriorly. Because the effects of *cwn-1(lf)* and *cwn-2(lf)* are mild (Gleason et al., 2006), we investigated the mechanisms by which *egl-20*, *lin-44*, and *mom-2* influence VPC orientation.

Wnt/EGL-20 Is Required for the Posterior-Facing or "Ground" Orientation of P5.p and P7.p

The above analysis suggested that Wnt/EGL-20 promotes P7.p orientation to face posteriorly. We next investigated whether EGL-20 is also involved in orienting P5.p posteriorly. We found that a small percentage of *lin-17(lf)*; *egl-20(lf); lin-18(lf)* triple mutants are A-Rvl (Figure 2C), a novel phenotype observed in neither *lin-17(lf); lin-18(lf)* nor *egl-20(lf)* mutants (Table 1). In addition, some of these triple mutants displayed simultaneous reversals in both P5.p and P7.p (the AP-Rvl phenotype, Figure 2D). These results suggest that Fz/LIN-17, Ryk/LIN-18, and Wnt/EGL-20 function redundantly to orient P5.p posteriorly. The low penetrance of the A-Rvl phenotype might be due to Wnt/CWN-1 activity, which weakly promotes the posterior-facing orientation in P7.p. On the basis of these results, we propose that Wnt/EGL-20 acts as a global cue to establish a uniform underlying polarity, which we call "ground" polarity, in which both P5.p and P7.p face posteriorly (Figure 2E, see below).

Default Orientation in the Absence of Wnts

That 50% of *Fz/lin-17(lf)*; *Wnt/egl-20(lf); Ryk/lin-18(lf)* triple mutants are P-Rvl suggested a model in which P5.p and P7.p orient randomly along the AP axis in the absence of all Wnt signaling

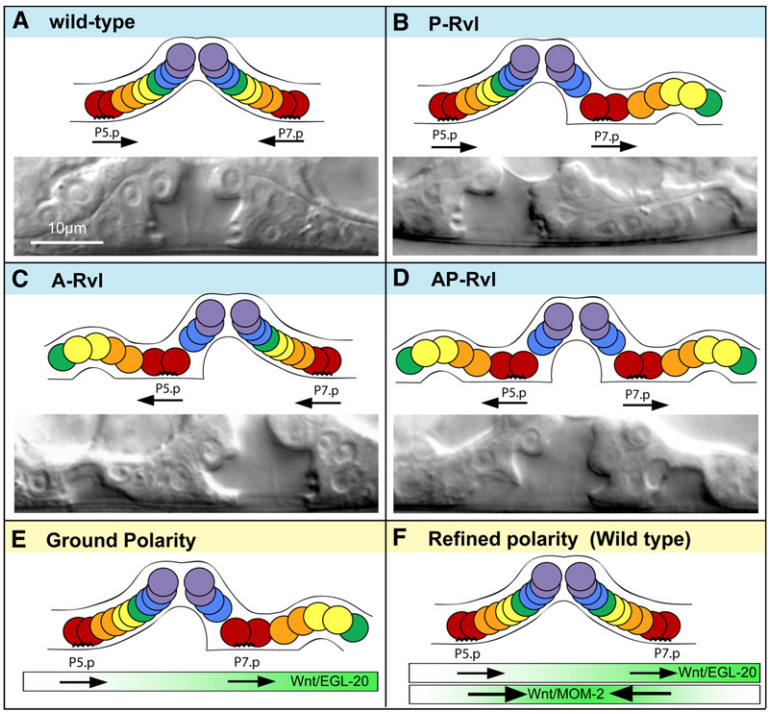

Figure 2. Vulval Lineage Orientations and Layered Polarity Model

Schematic arrangements of vulval lineages (top) and an example Nomarski image (bottom) for the four possible orientation combinations of P5.p and P7.p. Anterior, left.

(A) Wild-type; P5.p faces posteriorly, and P7.p faces anteriorly.

(B) P-Rvl; both P5.p and P7.p face posteriorly.

(C) A-Rvl; both P5.p and P7.p face anteriorly.

(D) AP-Rvl; P5.p faces anteriorly, and P7.p faces posteriorly.

(E) EGL-20, expressed from the posterior, promotes both P5.p and P7.p to face posteriorly.

(F) MOM-2, expressed in the centrally located anchor cell, orients both P5.p and P7.p toward the center. MOM-2 reverses P7.p polarity so that it faces anteriorly and reinforces the posterior-facing orientation of P5.p.

(true default). However, lethality of *Wnt/mom-2(lf)* mutant worms and lack of a vulva in *cwn-1(lf)*; *egl-20(lf)* double mutants (Gleason et al., 2006) prevented us from analyzing P7.p orientation in quintuple Wnt (*lin-44*, *cwn-1, egl-20, cwn-2, mom-2*) mutants. We therefore used heat-shock-controlled overexpression of Ror/CAM-1 (*hs::CAM-1*) (Figure S1 available online), which sequesters Wnts (Green et al., 2007), as an inducible method of eliminating Wnt activity (see the Supplemental Data for controls). Inducement of CAM-1 overexpression after vulval induction and before polarity specification caused all four polarity outcomes predicted to occur in the absence of Wnt signaling: A-Rvl, P-Rvl, AP-Rvl, and wild-type (Table 1). Consistent with the result that the CAM-1 cysteine-rich domain (CRD) binds to CWN-1, EGL-20, and MOM-2 in vitro, but not to LIN-44 (Green et al., 2007), these phenotypes became more penetrant in a *Wnt/lin-44(lf)* mutant background. The most severe phenotype, AP-Rvl, is underrepresented, possibly because of residual Wnt activity. Analysis of cell-type-specific markers *ceh-2::YFP* and *cdh-3::CFP* (Deshpande et al., 2005; Inoue et al., 2002) confirmed that the phenotype is indeed due to a patterning defect and not a migration defect (data not shown). These results support the model in which VPCs orient randomly in the absence of Wnt signaling.

The Anchor Cell Is an Important Wnt Source during VPC Orientation

Although Wnt/LIN-44 and Wnt/MOM-2 are redundantly required to reorient P7.p (Gleason et al., 2006; Inoue et al., 2004), their relevant site of expression is not clear. In addition to other tissues, *mom-2* and *lin-44* are expressed in the anchor cell (AC) at the axis of symmetry (Figure S2B) (Inoue et al., 2004), suggesting that Wnts might function as centrally orienting cues. To test this, we interfered with Wnt activity from the AC by expressing CAM-1::GFP specifically in the AC membrane (*Pfos-1a::CAM-1::GFP*) using the AC-specific promoter *Pfos-1a* (Sherwood et al., 2005) (Figure S2C). Because Ror/CAM-1 can sequester Wnts and appears to bind to MOM-2, but not to LIN-44, in vitro (Green et al., 2007), we reasoned that expression of this construct would antagonize MOM-2 expressed from the AC and therefore confer a P-Rvl phenotype to *lin-44(lf)* mutants. Consistently, we observed a 46% P-Rvl phenotype in *lin-44(lf); Pfos-1a::CAM-1::GFP* animals (Table 1). Supported by control experiments (see the Supplemental Data), these results indicate that MOM-2 (and possibly Wnt/LIN-44) expressed from the AC acts as a local cue to orient P5.p and P7.p toward the center, which we call "refined" polarity (Figure 2F, see below).

EGL-20 Acts Instructively

egl-20 is expressed in the tail (Whangbo and Kenyon, 1999) and forms a posterior-to-anterior concentration gradient (Coudreuse et al., 2006), suggesting that EGL-20 functions instructively (imparts directional information) rather than permissively (does not provide directional information but is required for polarization). However, there is precedent for EGL-20 having both types of activity (Pan et al., 2006; Whangbo and Kenyon, 1999). To discriminate between these possibilities, we tested whether changing the direction of the EGL-20 gradient affects VPC orientation. We first expressed *egl-20* broadly using the heat-shock promoter (*Phs::EGL-20*). If EGL-20 acts permissively, *Phs::EGL-20* expression should restore the P-Rvl phenotype of *lin-17(lf)*; *egl-20(lf)* double mutants [i.e., restore the *lin-17(lf)* phenotype]. On the other hand, if EGL-20 is an instructive cue, then *Phs::EGL-20* expression in *lin-17(lf)*; *egl-20(lf)* double mutants should result in all four VPC phenotypes: P-Rvl, A-Rvl, AP-Rvl, and WT. We observed all four phenotypes upon heat shock, consistent with instructive EGL-20 function (Table 1).

To further assess whether EGL-20 acts instructively or permissively, we moved the source of *egl-20* expression from the posterior to the anterior side of P7.p. Although we were unable to reverse the EGL-20 gradient over the entire length of the worm (see the Supplemental Data), we used *Pfos-1a* to express

Table 1. Reversed Vulval Lineage Phenotype

Relevant Genotype	% P-Rvl	% A-Rvl	% AP-Rvl	n	p Value
lin-17(n671)	74	0	0	113	
lin-18(e620)	36	0	0	113	
*lin-17(n671); lin-18(e620)**	100	0	0	63	
egl-20(n585)	0	0	0	22	
lin-17(n671); egl-20(n585)	8	0	0	64	<0.0001[a]
egl-20(n585); lin-18(e620)	7	0	0	70	<0.0001[b]
egl-20(hu120)	0	0	0	66	
lin-17(n671); egl-20(hu120)	6	0	0	52	<0.0001[a]
egl-20(hu120); lin-18(e620)	8	0	0	51	<0.0001[b]
lin-17(n671); egl-20(n585); lin-18(e620)	48	6	2	66	<0.0001[c]
lin-17(n671); egl-20(hu120); lin-18(e620)	50	2	0	52	<0.0001[c]
cwn-1(ok546)	0	0	0	38	
lin-17(n671); cwn-1(ok546)	52	0	0	54	0.005[a]
cwn-1(ok546); lin-18(e620)	26	0	0	53	0.222[b]
lin-17(n671); cwn-1(ok546); lin-18(e620)	92	0	0	47	0.075[c]
parent strain[#]	0	0	0	40	
syEx710[Pheat-shock::CAM-1][#]	12	14	2	59	<0.0001[d]
lin-44(n1792); syEx710[Pheat-shock::CAM-1][#]	43	35	8	84	<0.0001[e]
*mom-2(or42)**	1	0	0	83	
*lin-44(n1792)**	0	0	0	120	
*lin-44(n1792); mom-2(or42)**	59	0	0	127	<0.0001[e]
syEx780[Pfos-1a::CAM-1::GFP]	0	0	0	21	
syEx777[Pfos-1a::CAM-1::GFP]	0	0	0	21	
lin-44(n1792); syEx780[Pfos-1a::CAM-1::GFP]	46	2	2	54	<0.0001[e]
lin-17(n671); egl-20(hu120)[#]	0	0	0	51	
lin-17(n671); egl-20(hu120); syEx1024[Pheat-shock::EGL-20][#]	75	54	46	28	
lin-17(n671); egl-20(hu120); syEx1025[Pheat-shock::EGL-20][#]	76	48	33	21	
lin-17(n671); egl-20(hu120); lin-18(e620); syEx1031[Pfos-1a::EGL-20::GFP]	13	0	0	23	0.002[f]
lin-17(n671); syEx1031[Pfos-1a::EGL-20::GFP]	25	0	0	44	<0.0001[a]
pop-1(q645)	0	0	0	18	
pop-1(RNAi)	3	0	0	39	
sys-1(q544)	2	0	0	44	
wrm-1(ne1982)	4	4	0	23	
lit-1(or131)	0	0	0	22	
lin-17(n671); lit-1(or131)	11	6	0	36	<0.0001[a]
lit-1(or131); lin-18(e620)	17	0	0	64	0.010[b]
bar-1(ga80)	0	0	0	20	
sys-1(q544); bar-1(ga80)	15	3	0	40	
vang-1(ok1142)	0	0	0	58	
lin-17(n671); vang-1(ok1142)	48	3	3	60	0.005[a]
lin-17(n671); egl-20(hu120); vang-1(ok1142)	2	0	0	50	
lin-17(n671); vang-1(ok1142); syEx1031[Pfos-1a::EGL-20::GFP]	46	0	0	71	0.030[g]
cam-1(gm122)	0	0	0	54	
lin-17(n671); cam-1(gm122)	46	2	0	54	0.005[a]
cam-1(sa692)	0	0	0	50	
lin-17(n671); cam-1(sa692)	51	0	0	45	0.008[a]
cam-1(ak37)	0	0	0	53	
lin-17(n671); cam-1(ak37)	38	0	0	48	<0.0001[a]
cam-1(gm105)	0	0	0	54	
lin-17(n671); cam-1(gm105)	55	0	0	53	0.013[a]
cam-1(ks52)	0	0	0	53	
lin-17(n671); cam-1(ks52)	23	0	0	52	<0.0001[a]
lin-17(n671); cam-1(gm122); syEx1031[Pfos-1a::EGL-20::GFP]	52	4	0	23	0.033[g]
lin-17(n671); cam-1(gm122); vang-1(ok1142)	38	8	5	61	0.449[h]
lin-17(n671); cam-1(ks52); vang-1(ok1142)	28	2	2	53	0.656[i]
lin-17(n671); cam-1(gm122); egl-20(n585)	15	3	0	40	
lin-17(n671); cam-1(gm122); Ex[Psnb-1::CAM-1::GFP]	49	3	0	39	0.863[h]
lin-17(n671); cam-1(gm122); Ex[Pmyo-3::CAM-1::GFP]	55	0	0	20	0.604[h]
lin-17(n671); jnk-1(gk7)	74	2	0	43	1.0[a]

For each genotype, only worms with wild-type vulval induction, i.e., 3.0, were scored. *pop-1(q645), sys-1(q544)* and *mom-2(or42)* are homozygous progeny from heterozygous mothers. *lit-1(or131)* and *wrm-1(ne1982)* are temperature-sensitive alleles; L1 worms were raised at 25°C. AP-Rvl worms are also included in A-Rvl and P-Rvl categories. * indicates values originally reported in Inoue et al. (2004). # indicates mixed-stage worms that were heat-shocked 45 min (CAM-1) or 20 min (EGL-20) at 33°C; mid-L4 animals were scored 16 hr later.

[a] Compared to *lin-17(n671)* with Fisher's exact test.

[b] Compared to *lin-18(e620)* with Fisher's exact test.

[c] Compared to *lin-17(n671); lin-18(e620)* with Fisher's exact test.

[d] Compared to *pha-1(e2123);him-5(e1490)* with Fisher's exact test.

[e] Compared to *lin-44(n1792)* with Fisher's exact test.

[f] Compared to *lin-17(n671); egl-20(hu120); lin-18(e620)* with Fisher's exact test.

[g] Compared to *lin-17(n671); syEx1031[Pfos-1a::EGL-20::GFP]* with Fisher's exact test.

[h] Compared to *lin-17(n671); cam-1(gm122)* with Fisher's exact test.

[i] Compared to *lin-17(n671); cam-1(ks52)* with Fisher's exact test.

egl-20 from the AC, anterior to P7.p. We expressed *Pfos-1a::EGL-20::GFP* in *Fz/lin-17*; *Wnt/egl-20; Ryk/lin-18* triple mutants, which are 50% P-Rvl. If EGL-20 is a permissive cue, then *Pfos-1a::EGL-20::GFP* should restore the P-Rvl phenotype of these worms to 100%, as in *Fz/lin-17*; *Ryk/lin-18* double mutants. In contrast, instructive EGL-20 activity from the AC is expected to orient P5.p and P7.p toward the source of *egl-20*

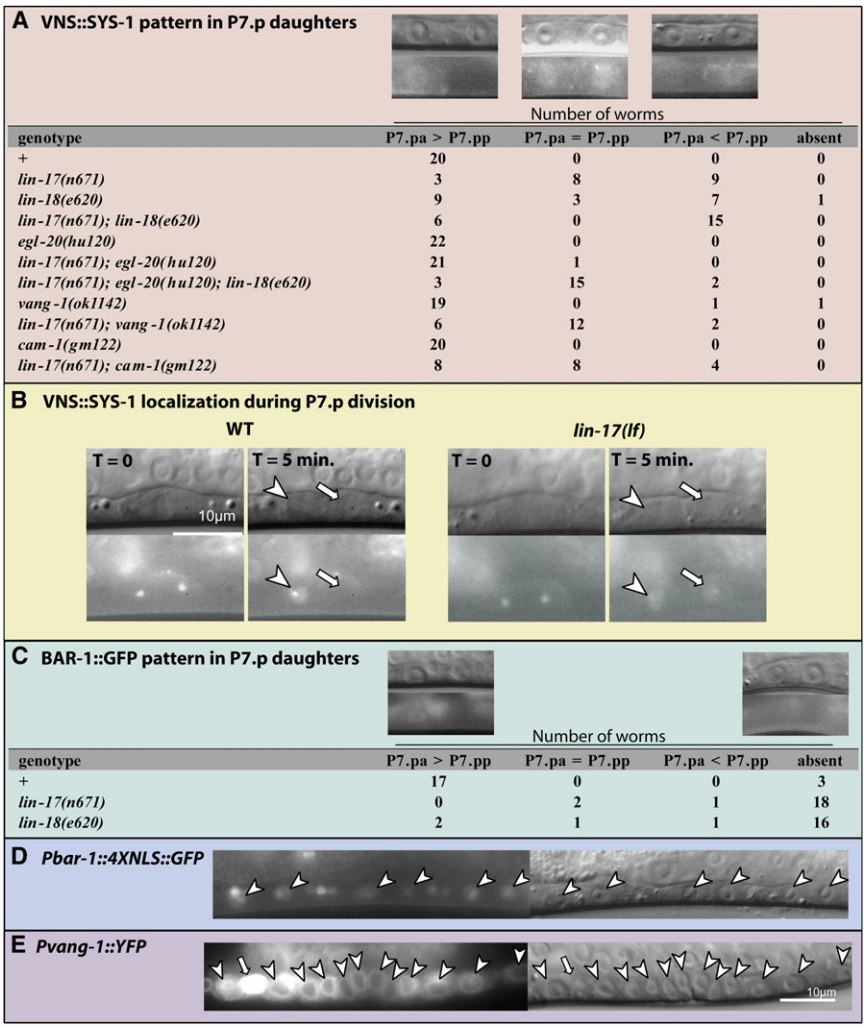

Figure 3. SYS-1, BAR-1, and VANG-1 Expression in VPC Progeny

(A) Subcellular localization of *qIs95*, a VNS::SYS-1 translational fusion. *qIs95* is expressed at very low levels. To characterize the localization, we captured a still fluorescence image using a long exposure time (8 s) and then applied the "Auto Contrast" function of Adobe Photoshop CS2. The resulting localization pattern was readily classifiable by eye into one of the three categories: SYS-1 was enriched in the anterior P7.p daughter nucleus (P7.pa > P7.pp), SYS-1 was present at similar levels in both P7.p daughter nuclei (P7.pa = P7.pp), or SYS-1 was enriched in the posterior P7.p daughter nucleus (P7.pa < P7.pp). A representative image is shown above each category, and the number of worms in each category is listed. The VNS::SYS-1 localization pattern in P5.p daughters was unaffected in all of the genotypes examined, with the exception of symmetric distribution in a single *lin-17(lf); egl-20(lf)* double-mutant worm and in two *lin-17(lf); egl-20(lf); lin-18(lf)* triple mutants.

(B) Nomarski (above) and fluorescence (below) images show VNS::SYS-1 localization during cell division. For the wild-type and *lin-17(lf)* mutants, the images on the right were taken 5 min after the images on the left. The two spots seen in the fluorescent images on the left are putative centrosomes. Arrowheads point to anterior daughter nuclei, and arrows point to posterior daughter nuclei.

(C) BAR-1::GFP translation fusion; display is the same as in (A).

(D) A *bar-1::GFP* reporter that contains 5.1 kb of the *bar-1* 5′ regulatory region driving expression of nucleolus/nuclear-localized GFP. This promoter region is the same as in (C) (Eisenmann et al., 1998).

(E) *vang-1::YFP* reporter is expressed in the VPC progeny (arrowheads). The bright *vang-1::YFP*-expressing cell (arrow) is a ventral cord neuron.

expression and thus rescue the 50% P-Rvl phenotype to the wild-type. Expression of *Pfos-1a::EGL-20::GFP* rescued the P-Rvl phenotype (Table 1), consistent with an instructive function. We next tested whether *Pfos-1a::EGL-20::GFP* could compete with endogenous *egl-20* when expressed in *lin-17(lf)* single mutants. *Pfos-1a::EGL-20::GFP* rescued the *lin-17(lf)* phenotype; therefore, P7.p orients toward higher levels of EGL-20. Together, these results indicate that reversing the EGL-20 gradient can reverse the ground polarity of the VPCs.

Wnt/β-catenin Asymmetry Pathway Components

To begin to distinguish the molecular mechanisms by which spatially resolved Wnts exert opposing effects on cell polarity, we investigated the involvement of potential downstream components. Wnt signals are often transduced by β-catenin, and three *C. elegans* β-catenin-related proteins, SYS-1, WRM-1, and BAR-1, function in two distinct pathways. BAR-1 functions as a classic β-catenin and will be discussed later. SYS-1 and WRM-1 are components of the Wnt/β-catenin asymmetry pathway, which also includes TCF/POP-1 and Nemo-like-kinase/LIT-1. The Wnt/β-catenin asymmetry pathway ensures different ratios of SYS-1 to POP-1, and thus differential transcription of Wnt target genes, between daughters of an asymmetric cell division (reviewed by Mizumoto and Sawa, 2007). In many tissues, POP-1 asymmetry is generated by WRM-1 and LIT-1, which together promote nuclear export of POP-1 (Lo et al., 2004; Maduro et al., 2002). POP-1 is asymmetrically localized between P7.p daughter nuclei in a low (P7.pa)/high (P7.pp) pattern (Deshpande et al., 2005). GFP::LIT-1 (Rocheleau et al., 1999) and WRM-1::GFP (Takeshita and Sawa, 2005) are localized in a reciprocal pattern to POP-1 in P7.p daughter nuclei (Figure S3), indicating that the relationship between POP-1, WRM-1, and LIT-1 in the VPCs is similar to that in other tissues. A rescuing fluorescent SYS-1 fusion protein (VNS::SYS-1) is also asymmetrically localized in a high (P7.pa)/low (P7.pp) pattern reciprocal to POP-1 (Figure 3A) (Phillips et al., 2007). By monitoring VNS::SYS-1 localization during division, we confirmed that this asymmetry reflects the orientation of the parent cell rather than signaling to P7.p daughters immediately after division (Figure 3B) (see the Supplemental Data).

As reported for the somatic gonadal precursors (SGPs) in *Fz* mutants (Phillips et al., 2007), VNS::SYS-1 asymmetry in P7.p

daughters was sometimes lost in *lin-17(lf)* mutants (Figures 3A and 3B). We additionally observed a loss of VNS::SYS-1 asymmetry in *lin-18(lf)* mutants, indicating that Ryk/LIN-18 also controls VNS::SYS-1 asymmetry. Unlike in the SGPs, in the VPCs, *lin-17(lf)* and *lin-18(lf)* mutants also frequently displayed a reversed VNS::SYS-1 localization pattern in which VNS::SYS-1 was enriched in P7.pp instead of P7.pa, suggesting the presence of an additional factor that controls SYS-1 asymmetry and promotes the opposite pattern, i.e., low (P7.pa)/high (P7.pp). Our analysis of the P-Rvl phenotype suggested that EGL-20 promotes the posterior orientation of P7.p. Consistently, *egl-20(lf)* drastically suppressed the VNS::SYS-1 localization defects caused by *lin-17(lf)*, confirming that EGL-20 promotes reversed VNS::SYS-1 localization in P7.p daughters. In *lin-17(lf); lin-18(lf)* double mutants, VNS::SYS-1 localization defects consisted only of reversals with no case of symmetric distribution observed. *egl-20(lf)* suppressed the reversed VNS::SYS-1 phenotype of *lin-17(lf); lin-18(lf)* double mutants such that the majority of triply mutant worms now displayed symmetric localization of VNS::SYS-1 between P7.p daughter nuclei. These results show that EGL-20 promotes the reversed localization of VNS::SYS-1 in the absence of the LIN-17 and LIN-18 branches of Wnt signaling and that in the absence of all three branches of Wnt signaling, VNS::SYS-1 asymmetry is lost. VNS::SYS-1 asymmetry, however, is not the only determinant of VPC orientation. Although 75% of *lin-17(lf); egl-20(lf); lin-18(lf)* triple mutants displayed symmetric VNS::SYS-1 localization, only 50% displayed the P-Rvl phenotype, and no cases were observed in which anterior and posterior halves of the P7.p-derived tissue were symmetric. Thus one explanation for these results is that symmetric VNS::SYS-1 localization is an intermediate phenotype in which P7.p randomly adopts either orientation.

Curiously, occurrence of the P-Rvl phenotype in *pop-1*, *sys-1*, *wrm-1*, and *lit-1* mutants was rare (Table 1). This could indicate that they are not required for VPC orientation or that like *egl-20*, their involvement is masked in single-mutant worms. Consistent with the latter scenario, *lit-1(lf)* suppressed the P-Rvl phenotype of *lin-17(lf)* and *lin-18(lf)* mutants.

β-catenin Function during VPC Orientation

Although they function in different pathways, both SYS-1 and BAR-1, a classic β-catenin, can function as transcriptional coactivators with TCF/POP-1, raising the possibility of redundancy (Kidd et al., 2005; Korswagen et al., 2000). While *bar-1(lf)* mutants did not display VPC polarity defects (Table 1), 15% of *sys-1(rf); bar-1(lf)* double mutants were P-Rvl, indicating that *sys-1* and *bar-1* play a minor redundant role in P7.p reorientation. We attempted to test whether β-catenin/WRM-1 was also functionally redundant with SYS-1 and BAR-1; however, all *wrm-1(rf); bar-1(lf)* double mutants examined (n = 28) were vulvaless because of an earlier requirement for β-catenin in vulval induction, and they therefore could not be scored. Because BAR-1 appeared to play a minor role in VPC orientation, we examined BAR-1 localization in the VPC progeny. In wild-type animals, BAR-1::GFP (Eisenmann et al., 1998) is localized asymmetrically, with higher nuclear levels in the proximal daughters of P5.p and P7.p (Figure 3C). Asymmetric distribution of BAR-1 after division had not previously been described; therefore, we tested whether BAR-1 asymmetry is generated by regulation of BAR-1 protein or by unequal transcription by making a *bar-1* transcriptional reporter (*Pbar-1::4XNLS::GFP*) that has the same 5.1 kb promoter sequence as the BAR-1::GFP fusion protein. Unlike BAR-1::GFP, *Pbar-1::4XNLS::GFP* was expressed at equivalent levels in both daughters of P5.p and P7.p, suggesting that BAR-1 asymmetry is regulated at the protein level (Figure 3D). We next tested whether *Fz/lin-17(lf)* or *Ryk/lin-18(lf)* is required for BAR-1 asymmetry. In *Fz/lin-17(lf)* and *Ryk/lin-18(lf)* mutants, BAR-1::GFP was no longer enriched in either daughter nucleus. Thus, BAR-1 asymmetry is different than SYS-1 asymmetry, which is reversed in *lin-17(lf)* and *lin-18(lf)* mutants. We conclude that Fz/LIN-17 and Ryk/LIN-18 regulate the localization of BAR-1 protein by increasing its level in the proximal daughter nuclei and that unlike SYS-1 localization, BAR-1 localization in the VPC daughters is not regulated by EGL-20. Because nuclear enrichment of β-catenin is expected to regulate the transcription of Wnt target genes, we next investigated whether Wnt pathway targets are expressed during P7.p reorientation.

Fz/LIN-17 and Ryk/LIN-18 Regulate POPTOP Expression in the VPC Progeny

Wnt signaling activity is commonly measured in vitro with the TOPFLASH reporter, consisting of multiple TCF binding sites driving expression of luciferase (Molenaar et al., 1996; van de Wetering et al., 1997). To measure TCF/POP-1 activity in vivo, we made an analogous *C. elegans* reporter, POPTOP (*POP*-1 and *T*CF *o*ptimal *p*romoter), that contains seven copies of the TCF/POP-1 binding site and a minimal promoter driving expression of the fluorescent protein *mCherry* (McNally et al., 2006). Control experiments showed that POPTOP expression reflects POP-1-induced gene expression (see the Supplemental Data). In wild-type worms, POPTOP is expressed at low levels in the proximal, but not distal, daughters of P5.p and P7.p and at moderate and equal levels in the proximal granddaughters of P5.p and P7.p (Figure 4, Tables S2 and S3). POPTOP expression is reciprocal to POP-1 localization after the first division, (Deshpande et al., 2005), which is consistent with reports that TCF/POP-1, while functioning as an activator at low levels, functions as a repressor when present in the nucleus at high levels (Shetty et al., 2005).

POPTOP expression in the VPC progeny was elevated upon removal of *Axin/pry-1* (a negative regulator of Wnt signaling) and was eliminated in *pop-1* mutants, confirming that POPTOP is regulated by Wnt signaling (Figure 4, Table S3). Both *β-catenins sys-1* and *bar-1* are expressed in a pattern that would allow them to serve as a transcriptional coactivator with TCF/POP-1 (Figures 3A and 3C); therefore, we examined POPTOP expression in *bar-1(lf)* and *sys-1(rf)* mutant worms. POPTOP expression in P7.p granddaughters was reduced, though not significantly, in *sys-1(rf)* and *bar-1(lf)* mutants (Table S3), demonstrating that SYS-1 and BAR-1 probably function redundantly to activate Wnt target genes in these cells. In *lin-17(lf)* and *lin-18(lf)* mutants, POPTOP expression in the VPC progeny was eliminated, indicating that Fz/LIN-17 and Ryk/LIN-18 activate POP-1-mediated transcription in the proximal daughters of P5.p and P7.p. *egl-20(lf)*, which rescues the *lin-17(lf)* P-Rvl phenotype, does not restore POPTOP expression in *lin-17(lf); egl-20(lf)* double mutants

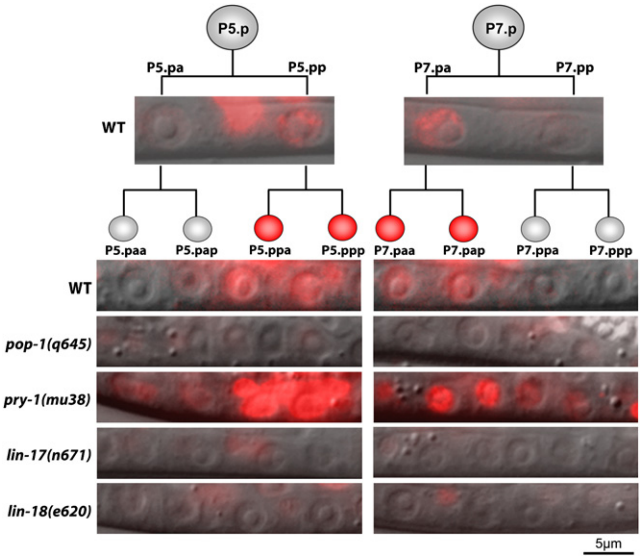

Figure 4. POPTOP Expression in VPC Granddaughters

Overlay of Nomarski and fluorescence (red) images showing POPTOP expression in the VPC progeny. Representative images are shown. Fluorescent images of the VPC granddaughters were each exposed for 1 s, except for *pry-1(mu38)*, which was exposed for 0.5 s. The fluorescence remaining in *lin-17(lf)* and *lin-18(lf)* mutants is in ventral cord neurons, where POPTOP is also expressed.

(Table S3), suggesting that refined polarity is largely independent of POP-1-mediated transcriptional activation. That POPTOP expression was eliminated in *lin-17(lf)* and *lin-18(lf)* mutants, instead of being reversed, indicates that POPTOP is not influenced by ground polarity signaling.

Van Gogh/VANG-1 Functions in Ground Polarity

Besides appearing independent of transcription, ground polarity presented an enigma because the receptor for EGL-20 was unknown. Loss of the receptor for EGL-20 should mimic loss of *egl-20* and also suppress the P-Rvl phenotype of *lin-17(lf)* worms. However, the three remaining Fz receptors promote anterior P7.p orientation, and their removal (by mutation or RNAi) does not suppress the *lin-17(lf)* P-Rvl phenotype (Gleason et al., 2006). This suggests that EGL-20 acts via an alternative mechanism. We therefore considered PCP, another mechanism of cellular orientation in which Fz can act positively or negatively.

VPC orientation bears the hallmark of PCP: the polarization of an epithelial tissue along the plane of the cell layer, perpendicular to the apical-basal axis of the cells comprising the epithelium. In *Drosophila* and vertebrates, PCP is regulated by a core set of PCP pathway components, including Frizzled, Van Gogh, Prickle, and Flamingo (recently reviewed by Jones and Chen, 2007; Seifert and Mlodzik, 2007; Wang and Nathans, 2007; Zallen, 2007). Also like PCP, VPC orientation does not appear to depend on gene transcription. Although the PCP pathway has not been clearly demonstrated in *C. elegans*, the resemblance of VPC orientation to PCP raised the possibility that PCP components might be involved. Thus, we tested for involvement of *Van Gogh/vang-1*, a PCP pathway-specific four-pass transmembrane protein that is conserved in *C. elegans* (Park et al., 2004). We first generated a *vang-1::YFP* reporter and observed expression in the VPC progeny (Figure 3E). Although *vang-1(lf)* worms did not display VPC polarity defects, we found that *vang-1(lf)* significantly suppressed the P-Rvl phenotype of *Fz/lin-17(lf)* worms (Table 1). *vang-1(lf)* also significantly suppressed the reversed VNS::SYS-1 localization pattern of *lin-17(lf)* worms, such that fewer animals displayed the reversed localization and an increased number had symmetric localization.

To test whether *vang-1* acts downstream of *egl-20* during the establishment of ground polarity, we ectopically expressed EGL-20 in the AC using *Pfos-1a::EGL-20:GFP*, which reduces the P-Rvl phenotype of *lin-17(lf)* worms. Upon removal of *vang-1*, *Pfos-1a::EGL-20:GFP* no longer reoriented P7.p toward the center (Table 1), indicating that *Van Gogh/vang-1* acts downstream of *egl-20* during VPC orientation (Figure 5A). *vang-1(lf)* suppression of *lin-17(lf)* is much weaker (50% P-Rvl) than the suppression seen with *egl-20(lf)* (6% P-Rvl). Additionally, the *lin-17(lf); egl-20(lf); vang-1(lf)* triple mutants (2% P-Rvl) were not significantly different than the *lin-17(lf); egl-20(lf)* double mutants, demonstrating that *egl-20* acts partly via *vang-1* and partly via another mechanism.

Ror/CAM-1 Functions in Ground Polarity

Van Gogh is a transmembrane protein without an obvious Wnt-binding domain. We therefore investigated how EGL-20 might activate VANG-1. Since none of the Fz and Ryk receptors were apparently required for ground polarity, we tested the only other known Wnt receptor in *C. elegans*, *Ror/cam-1*. Ror proteins are RTKs containing an extracellular Wnt-binding Frizzled (Fz) domain (also called cysteine-rich domain or CRD), an immunoglobulin (Ig) domain, and a Kringle domain (Figure 6). We previously showed that *cam-1*, the sole *C. elegans* Ror family member, is expressed in the VPCs and physically interacts with EGL-20 in vitro (Green et al., 2007). To investigate whether *cam-1* is involved in ground polarity, we tested whether the *cam-1(lf)* mutation, *gm122*, suppressed the *lin-17(lf)* P-Rvl phenotype. *cam-1(lf)* suppressed *lin-17(lf)* P-Rvl to 46%, similar to the suppression seen with *vang-1(lf)* (Table 1). *cam-1(lf)* also suppressed the VNS::SYS-1 localization defects of *lin-17(lf)* worms in a way similar to *vang-1(lf)*: fewer animals displayed the reversed localization, and an increased number had symmetric localization (Figure 3A). To test whether *cam-1* functions in the same pathway as *egl-20* and *vang-1*, we constructed *lin-17(lf); cam-1(lf or rf); vang-1(lf)* triple mutants using either of two different *cam-1* alleles. In both strains, the P-Rvl phenotype was not different from the *lin-17(lf); cam-1(rf or lf)* double mutants, indicating that *cam-1* and *vang-1* function in the same pathway. To confirm that CAM-1 acts in the same pathway as EGL-20 and VANG-1, we introduced *Pfos-1a::EGL-20:GFP* into *lin-17(lf); cam-1(lf)* worms. Like *vang-1(lf)*, removal of *cam-1* prevented *Pfos-1a::EGL-20:GFP* from reorienting P7.p. Together, these results indicate that *cam-1* functions in the same pathway as *egl-20* and *vang-1* (Figure 5A) and raise the interesting possibility that CAM-1 and VANG-1 may function as coreceptors for EGL-20.

CAM-1 can act nonautonomously by sequestering Wnts (Green et al., 2007), and we showed earlier that overexpression of CAM-1 can abolish ground polarity. To test whether the

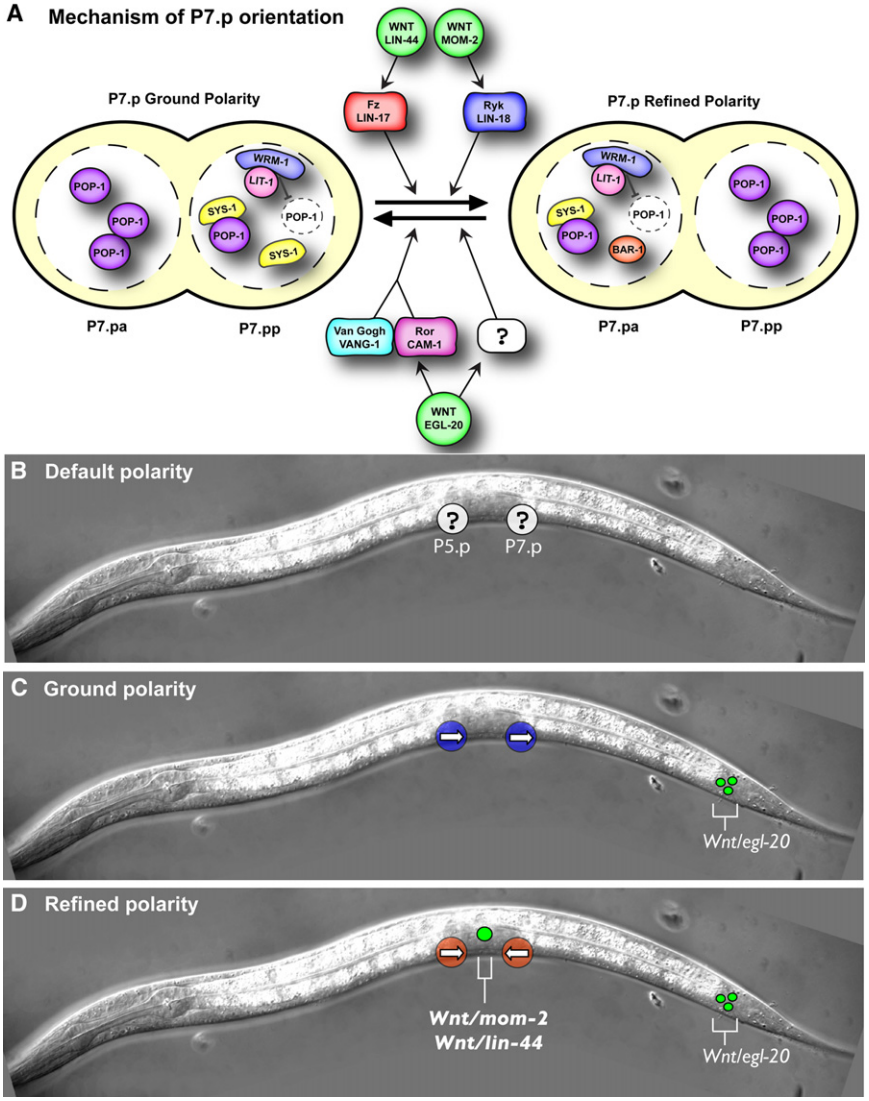

Figure 5. Model of VPC Orientation

(A) Illustration of the genetic interactions contributing to the orientation of P7.p and the nuclear localization of POP-1, WRM-1, LIT-1, SYS-1, and BAR-1 in ground and refined polarity. We have examined WRM-1 and LIT-1 localization in refined polarity, but WRM-1 and LIT-1 localization in ground polarity is inferred from POP-1 localization, which was previously described (Deshpande et al., 2005). Localization of SYS-1 and BAR-1 in ground and refined polarity was described here.

(B–D) Schematics of default, ground, and refined polarity. In the absence of Wnts, the orientation of P5.p and P7.p (white circles) is random (represented by a question mark) (B). *egl-20/Wnt* is expressed in the tail (green circles) and establishes ground polarity in which both P5.p and P7.p (blue circles) face posteriorly (arrows) (C). Wnts *mom-2* and *lin-44* are expressed in the AC (big green circle) and instruct P5.p and P7.p (red circles) to face the center (arrows) (D).

function of CAM-1 in ground polarity [*lin-17(lf)* suppression] is distinct from the Wnt-sequestration function, we used the five available *cam-1* mutant alleles to perform structure-function analysis (Figure 6). All five *cam-1* alleles examined suppressed the *lin-17(lf)* P-Rvl phenotype, including a missense mutation in the Wnt-binding domain (*sa692*) and a deletion of the intracellular kinase domain (*ks52*) (Table 1). Therefore, membrane insertion of a functional CRD, which is sufficient for sequestration (Supplemental Data) (Green et al., 2007), is not sufficient for CAM-1 function in ground polarity, suggesting a requirement for the CAM-1 intracellular domain and thus a cell-autonomous site of action. Also consistent with a cell-autonomous role, expression of CAM-1 in muscles (*myo-3* promoter) or neurons (*snb-1* promoter) (Green et al., 2007) did not restore the P-Rvl phenotype.

Since vertebrate Ror proteins activate c-Jun N-terminal kinase (JNK) in response to Wnt5a (Oishi et al., 2003; Schambony and Wedlich, 2007), we tested whether *jnk-1*, the *C. elegans* JNK ortholog, acts in the same pathway as *cam-1* during VPC orientation. *jnk-1(lf)* did not suppress the *lin-17(lf)* P-Rvl phenotype (Table 1), indicating that *jnk-1* is not required for *cam-1* to establish ground polarity.

DISCUSSION

Our results describe the contributions of multiple Wnt pathways to the orientation of cell polarity in the *C. elegans* vulval epithelium (Figure 5A). Because no factor required for the posterior orientation of P5.p or P7.p had previously been identified, this orientation was thought to be signaling independent or "default." However, when a new approach was used to reduce Wnt levels in a spatiotemporally controlled manner (overexpression of Ror/CAM-1, a Wnt sink), the VPCs displayed instead a randomized orientation, which is likely to be the true default (Figure 5B). The posterior orientation seen in the absence of *Fz/lin-17* and *Ryk/lin-18* depends on the instructive activity of Wnt/EGL-20. We refer to this polarity as "ground" polarity (Figures 2E and 5C). In response to centrally located Wnt/MOM-2 (and possibly Wnt/LIN-44), the receptors Fz/LIN-17 and Ryk/LIN-18 orient P5.p and P7.p toward the center. This reorientation of P7.p, "refined" polarity, provides the mirror-image symmetry required for a functional organ (Figures 2F and 5D).

That P7.p is oriented toward the center in wild-type worms suggests that Wnts LIN-44 and MOM-2 have a greater ability to affect P7.p orientation than does EGL-20. Although the posterior-anterior EGL-20 gradient reaches the VPCs, EGL-20 levels may be much lower here than the levels of Wnts secreted from the nearby AC (Coudreuse et al., 2006). Indeed, we found

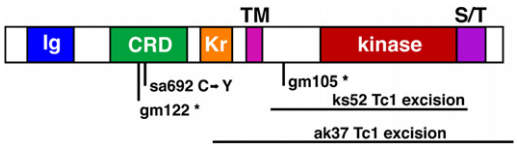

Figure 6. Ror/CAM-1 Structure and Molecular Lesions of Mutations
CAM-1 protein structure depicting immunoglobulin (Ig) domain, cysteine-rich domain (CRD), kringle domain (Kr), transmembrane (TM) domain, kinase domain, and serine/threonine-rich (S/T) domain. The amino terminus is to the left. The molecular nature of *cam-1* mutant alleles is given below.

that local expression of *egl-20* in the AC can overcome the effects of distally expressed *egl-20*. *lin-44* is expressed in the tail (Herman et al., 1995) in addition to the AC but has not been shown to have long-range activity. It is thus possible that this posterior source of *lin-44* does not affect P7.p orientation and that LIN-44, in addition to MOM-2, acts as a central cue.

LIN-17 and LIN-18 were previously reported to reorient P7.p and to reverse the AP pattern of nuclear TCF/POP-1 levels in P7.p daughters (Deshpande et al., 2005; Inoue et al., 2004). We extended our knowledge of the signaling downstream of Fz/LIN-17 and Ryk/LIN-18 by showing that these receptors control the asymmetric localization of two β-catenins, SYS-1 and BAR-1, the first evidence that Ryk proteins regulate β-catenin. Although asymmetric localization of SYS-1 suggests involvement of the Wnt/β-catenin asymmetry pathway, disruption of pathway components either did not cause a P-Rvl phenotype (*lit-1(rf)*) or caused only a weakly penetrant P-Rvl phenotype [*pop-1(RNAi), sys-1(rf),* and *wrm-1(rf)*], making the function of the Wnt/β-catenin asymmetry pathway in refined polarity unclear. We also showed that LIN-17 and LIN-18 activate transcription in the proximal VPC daughters. Yet, this transcription is not required for P7.p reorientation, since transcriptional states observed by POPTOP, a reporter of Wnt target genes, do not always correspond with the morphological phenotype. Therefore, refined polarity may be largely independent of BAR-1 or the Wnt/β-catenin asymmetry pathway and instead be analagous to the spindle reorientation of the EMS cell during *C. elegans* embryogenesis, in which Wnt signaling affects the cytoskeleton independent of Wnt's effect on gene expression (Schlesinger et al., 1999).

What then, is the purpose of the Wnt/β-catenin asymmetry pathway in the VPCs? The weakly penetrant A-Rvl phenotype seen in *wrm-1(rf)* and *lin-17(lf); lit-1(lf)* worms, combined with our observation that EGL-20 regulates SYS-1 asymmetry, suggests that the Wnt/β-catenin asymmetry pathway functions in ground polarity. Therefore, both ground and refined polarity may converge on regulation of these components, although they are not absolutely required for refined polarity. Because the localization of Wnt/β-catenin asymmetry pathway components in ground polarity matches the reiterative pattern seen in most other asymmetric cell divisions in *C. elegans* (Huang et al., 2007), we hypothesize that localization of these components is initially established as part of a global anterior-posterior polarity. It is likely that LIN-17 and LIN-18 overcome ground polarity by inhibiting the Wnt/β-catenin asymmetry pathway, a scenario consistent with the ability of *lit-1(rf)* to suppress *lin-17(lf)* and *lin-18(lf)* mutations.

Remarkably, it is only by peeling back the layer of refined polarity that ground polarity can be observed and manipulated. By doing so, we found that Wnt/EGL-20, expressed from a distant posterior source, imparts uniform AP polarity to the field of VPCs via a new pathway involving *Van Gogh/vang-1*, a core PCP pathway component. It is noteworthy that Fz is also a core PCP pathway component, yet it does not seem to be involved in EGL-20 signaling via VANG-1. This is not incompatible with other descriptions of PCP. For example, in the *Drosophila* wing, Van Gogh and Fz antagonize each other and cause wing hairs to orient in opposite directions (reviewed by Seifert and Mlodzik, 2007). The molecular mechanism by which VANG-1 functions in ground polarity is unknown; however, regulation of SYS-1 by VANG-1 provides evidence that the pathway involving *egl-20* and *vang-1* is associated with the Wnt/β-catenin asymmetry pathway.

A major difference between VPC orientation in *C. elegans* and PCP in *Drosophila* is that no Wnt has been directly implicated in *Drosophila* PCP. Therefore, VPC orientation may be more similar to some forms of PCP in vertebrates. For example, Wnts are believed to act as permissive polarizing factors during vertebrate convergent extension (Seifert and Mlodzik, 2007). Also, VPC orientation is strikingly similar to hair cell orientation in the utricular epithelia of the mammalian inner ear, wherein hair cells flanking the axis of symmetry are oriented in opposite directions (Deans et al., 2007). In this system, both medial and lateral hair cells possess a uniform underlying polarity as evidenced by asymmetric localization of Prickle, a core PCP pathway component, to the medial side of cells in both populations. Van Gogh is required for proper Prickle asymmetry, perhaps similarly to the role of *vang-1* in ground polarity of the VPCs. It is not understood how the position of the utricular axis of symmetry is determined, but the similarities between these two systems suggest that it may represent a local source of Wnt.

By moving the source of EGL-20 from the posterior to the anterior side of P7.p and thereby reversing P7.p orientation, we showed that EGL-20 acts as a directional cue. Although it is not presently clear if the pathway involving *egl-20* and *vang-1* is mechanistically similar to the PCP pathway described in *Drosophila* and vertebrates, our result nonetheless provides a long-sought example of a Wnt that acts instructively via a PCP pathway component. Detailed description of the subcellular localization of Van Gogh/VANG-1 and other PCP pathway components in the VPCs will be required to make meaningful comparisons between VPC orientation and established models of PCP.

In addition to *vang-1*, we also identified a role of *Ror/cam-1* in ground polarity. Our results provide the first evidence that Ror proteins interpret directional Wnt signals, as well as the first evidence that they interact with Van Gogh. Although a *Xenopus* Ror homolog, Xror2, was previously described to function in PCP during convergent extension (Hikasa et al., 2002), a recent report indicates that the involvement of Xror2 in convergent extension (CE) is actually via a different pathway (Schambony and Wedlich, 2007). In response to Wnt5a, Xror2 activates JNK by a mechanism requiring Xror2 kinase activity. In contrast to Wnt5a/Xror2

signaling, Ror/CAM-1 function in ground polarity does not require JNK. Therefore, the ground polarity pathway involving Wnt/EGL-20, Ror/CAM-1, and Van Gogh/VANG-1 may be a new type of Wnt signaling.

Using *C. elegans* vulva development as a model, we showed that multiple coexisting Wnt pathways with distinct ligand specificities and signaling mechanisms act in concert to regulate the polarity of individual cells during their assembly into complex structures.

EXPERIMENTAL PROCEDURES

Genetics

C. elegans was handled as described (Brenner, 1974). Strains used were derivatives of *C. elegans* N2 Bristol strain, which was the wild-type in this study. The following mutations were used: LGI: *lin-17(n671), pop-1(q645), lin-44(n1792), sys-1(q544)*; LGII: *cam-1(gm122, gm105, sa692, ks52, ak37), cwn-1(ok546)*; LGIII: *wrm-1(ne1982), lit-1(or131ts)*; LGIV: *jnk-1(gk7), egl-20(n585, hu120)*, *cwn-2(ok895)*; LGV: *mom-2(or42)*; and LGX: *vang-1(ok1142), lin-18(e620), bar-1(ga80)*. The *wrm-1(ne1982); bar-1(ga80)* double mutants were a kind gift from Craig Mello. P-Rvl and A-Rvl phenotypes were scored at the mid-L4 stage. Animals were classified as P-Rvl or A-Rvl if the primary and secondary VPCs were induced but separated by adherent cells. We consider the previously used description "bivulva" misleading because it implies the presence of extra vulval tissue and thus decided to call the phenotype Rvl for "*r*eversed *v*ulval *l*ineage."

Heat-Shock Ror/CAM-1

Worms carrying the *syEx710[Pheat-shock::CAM-1]* transgene were kept for 45 min at 33°C. Total lysates from heat-shocked, wild-type, and *cam-1(lf)* worms were separated by SDS-PAGE and probed with an anti-CAM-1 rabbit polyclonal antibody (B9851) that we raised (with BioSource International) against the C terminus (aa 858–928) of CAM-1 (C01G6.8a).

"POPTOP," *POP*-1 and *TCF Optimal P*romoter

Seven copies of the TCF binding site, AGATCAAAGG, were transferred from Super8XTOPflash (plasmid M50) (Veeman et al., 2003) into Fire lab vector L3135 (http://www.addgene.org) to place them upstream of the *pes-10* minimal promoter. The product was cloned into mCherry plasmid (PJIM20) with *let-858* 3′ UTR (kind gift from Jon Audhya) with sites SpeI and AvrII. The POPTOP plasmid was sequenced to confirm the integrity of the insert. POPFOP (*POP*-1 *f*ar from *o*ptimal *p*romoter) was made by a similar strategy using mutated TCF binding sites from plasmid Super8xFOPflash (plasmid M51). For details on POPTOP construction, characterization, and validation, see the Supplemental Data.

SUPPLEMENTAL DATA

Supplemental Data include Supplemental Results, three figures, three tables, and Supplemental References and can be found with this article online at http://www.cell.com/cgi/content/full/134/4/646/DC1/.

ACKNOWLEDGMENTS

We thank Gladys Medina, Barbara Perry, and Shahla Gharib for technical assistance, members of our lab for helpful discussions, Andrea Choe for artistic input, and Marianne Bronner-Fraser, Scott Fraser, Cheryl Van Buskirk, Mihoko Kato, Elissa Hallem, and Adeline Seah for critically reading the manuscript. Many strains used in this study were provided by the *Caenorhabditis* Genetics Center, funded by the National Institutes of Health, National Center for Research Resources. We are grateful to the late Peter Snow for his valuable assistance in making our CAM-1 antibody. P.W.S. is an investigator with the Howard Hughes Medical Institute, who supported this work, and J.L.G. was supported by the Moore Foundation Fellowship for graduate study toward the Doctor of Philosophy degree in Biology at the California Institute of Technology.

Received: October 30, 2007
Revised: April 23, 2008
Accepted: June 10, 2008
Published: August 21, 2008

REFERENCES

Baena-Lopez, L.A., Baonza, A., and Garcia-Bellido, A. (2005). The orientation of cell divisions determines the shape of Drosophila organs. Curr. Biol. *15*, 1640–1644.

Brenner, S. (1974). The genetics of Caenorhabditis elegans. Genetics *77*, 71–94.

Coudreuse, D.Y., Roel, G., Betist, M.C., Destree, O., and Korswagen, H.C. (2006). Wnt gradient formation requires retromer function in Wnt-producing cells. Science *312*, 921–924.

Deans, M.R., Antic, D., Suyama, K., Scott, M.P., Axelrod, J.D., and Goodrich, L.V. (2007). Asymmetric distribution of prickle-like 2 reveals an early underlying polarization of vestibular sensory epithelia in the inner ear. J. Neurosci. *27*, 3139–3147.

Deshpande, R., Inoue, T., Priess, J.R., and Hill, R.J. (2005). lin-17/Frizzled and lin-18 regulate POP-1/TCF-1 localization and cell type specification during C. elegans vulval development. Dev. Biol. *278*, 118–129.

Eisenmann, D.M., Maloof, J.N., Simske, J.S., Kenyon, C., and Kim, S.K. (1998). The beta-catenin homolog BAR-1 and LET-60 Ras coordinately regulate the Hox gene lin-39 during Caenorhabditis elegans vulval development. Development *125*, 3667–3680.

Ferguson, E.L., and Horvitz, H.R. (1985). Identification and characterization of 22 genes that affect the vulval cell lineages of the nematode Caenorhabditis elegans. Genetics *110*, 17–72.

Ferguson, E.L., Sternberg, P.W., and Horvitz, H.R. (1987). A genetic pathway for the specification of the vulval cell lineages of Caenorhabditis elegans. Nature *326*, 259–267.

Gleason, J.E., Szyleyko, E.A., and Eisenmann, D.M. (2006). Multiple redundant Wnt signaling components function in two processes during C. elegans vulval development. Dev. Biol. *298*, 442–457.

Gordon, M.D., and Nusse, R. (2006). Wnt signaling: Multiple pathways, multiple receptors, and multiple transcription factors. J. Biol. Chem. *281*, 22429–22433.

Green, J.L., Inoue, T., and Sternberg, P.W. (2007). The C. elegans ROR receptor tyrosine kinase, CAM-1, non-autonomously inhibits the Wnt pathway. Development *134*, 4053–4062.

Herman, M.A., Vassilieva, L.L., Horvitz, H.R., Shaw, J.E., and Herman, R.K. (1995). The C. elegans gene lin-44, which controls the polarity of certain asymmetric cell divisions, encodes a Wnt protein and acts cell nonautonomously. Cell *83*, 101–110.

Hikasa, H., Shibata, M., Hiratani, I., and Taira, M. (2002). The Xenopus receptor tyrosine kinase Xror2 modulates morphogenetic movements of the axial mesoderm and neuroectoderm via Wnt signaling. Development *129*, 5227–5239.

Huang, S., Shetty, P., Robertson, S.M., and Lin, R. (2007). Binary cell fate specification during C. elegans embryogenesis driven by reiterated reciprocal asymmetry of TCF POP-1 and its coactivator beta-catenin SYS-1. Development *134*, 2685–2695.

Inoue, T., Sherwood, D.R., Aspock, G., Butler, J.A., Gupta, B.P., Kirouac, M., Wang, M., Lee, P.Y., Kramer, J.M., Hope, I., et al. (2002). Gene expression markers for Caenorhabditis elegans vulval cells. Mech. Dev. *119* (*Suppl 1*), S203–S209.

Inoue, T., Oz, H.S., Wiland, D., Gharib, S., Deshpande, R., Hill, R.J., Katz, W.S., and Sternberg, P.W. (2004). C. elegans LIN-18 is a Ryk ortholog and functions in parallel to LIN-17/Frizzled in Wnt signaling. Cell *118*, 795–806.

Jones, C., and Chen, P. (2007). Planar cell polarity signaling in vertebrates. Bioessays *29*, 120–132.

Kidd, A.R., 3rd, Miskowski, J.A., Siegfried, K.R., Sawa, H., and Kimble, J. (2005). A beta-catenin identified by functional rather than sequence criteria and its role in Wnt/MAPK signaling. Cell *121*, 761–772.

Korswagen, H.C., Herman, M.A., and Clevers, H.C. (2000). Distinct beta-catenins mediate adhesion and signalling functions in C. elegans. Nature *406*, 527–532.

Lo, M.C., Gay, F., Odom, R., Shi, Y., and Lin, R. (2004). Phosphorylation by the beta-catenin/MAPK complex promotes 14–3-3-mediated nuclear export of TCF/POP-1 in signal-responsive cells in C. elegans. Cell *117*, 95–106.

Maduro, M.F., Lin, R., and Rothman, J.H. (2002). Dynamics of a developmental switch: recursive intracellular and intranuclear redistribution of Caenorhabditis elegans POP-1 parallels Wnt-inhibited transcriptional repression. Dev. Biol. *248*, 128–142.

McNally, K., Audhya, A., Oegema, K., and McNally, F.J. (2006). Katanin controls mitotic and meiotic spindle length. J. Cell Biol. *175*, 881–891.

Mizumoto, K., and Sawa, H. (2007). Two betas or not two betas: Regulation of asymmetric division by beta-catenin. Trends Cell Biol. *17*, 465–473.

Molenaar, M., van de Wetering, M., Oosterwegel, M., Peterson-Maduro, J., Godsave, S., Korinek, V., Roose, J., Destree, O., and Clevers, H. (1996). XTcf-3 transcription factor mediates beta-catenin-induced axis formation in Xenopus embryos. Cell *86*, 391–399.

Oishi, I., Suzuki, H., Onishi, N., Takada, R., Kani, S., Ohkawara, B., Koshida, I., Suzuki, K., Yamada, G., Schwabe, G.C., et al. (2003). The receptor tyrosine kinase Ror2 is involved in non-canonical Wnt5a/JNK signalling pathway. Genes Cells *8*, 645–654.

Pan, C.L., Howell, J.E., Clark, S.G., Hilliard, M., Cordes, S., Bargmann, C.I., and Garriga, G. (2006). Multiple Wnts and frizzled receptors regulate anteriorly directed cell and growth cone migrations in Caenorhabditis elegans. Dev. Cell *10*, 367–377.

Park, F.D., Tenlen, J.R., and Priess, J.R. (2004). C. elegans MOM-5/frizzled functions in MOM-2/Wnt-independent cell polarity and is localized asymmetrically prior to cell division. Curr. Biol. *14*, 2252–2258.

Phillips, B.T., Kidd, A.R., 3rd, King, R., Hardin, J., and Kimble, J. (2007). Reciprocal asymmetry of SYS-1/beta-catenin and POP-1/TCF controls asymmetric divisions in Caenorhabditis elegans. Proc. Natl. Acad. Sci. USA *104*, 3231–3236.

Rocheleau, C.E., Yasuda, J., Shin, T.H., Lin, R., Sawa, H., Okano, H., Priess, J.R., Davis, R.J., and Mello, C.C. (1999). WRM-1 activates the LIT-1 protein kinase to transduce anterior/posterior polarity signals in C. elegans. Cell *97*, 717–726.

Sawa, H., Lobel, L., and Horvitz, H.R. (1996). The Caenorhabditis elegans gene lin-17, which is required for certain asymmetric cell divisions, encodes a putative seven-transmembrane protein similar to the Drosophila frizzled protein. Genes Dev. *10*, 2189–2197.

Schambony, A., and Wedlich, D. (2007). Wnt-5A/Ror2 regulate expression of XPAPC through an alternative noncanonical signaling pathway. Dev. Cell *12*, 779–792.

Schlesinger, A., Shelton, C.A., Maloof, J.N., Meneghini, M., and Bowerman, B. (1999). Wnt pathway components orient a mitotic spindle in the early Caenorhabditis elegans embryo without requiring gene transcription in the responding cell. Genes Dev. *13*, 2028–2038.

Seifert, J.R., and Mlodzik, M. (2007). Frizzled/PCP signalling: A conserved mechanism regulating cell polarity and directed motility. Nat. Rev. Genet. *8*, 126–138.

Sherwood, D.R., Butler, J.A., Kramer, J.M., and Sternberg, P.W. (2005). FOS-1 promotes basement-membrane removal during anchor-cell invasion in C. elegans. Cell *121*, 951–962.

Shetty, P., Lo, M.C., Robertson, S.M., and Lin, R. (2005). C. elegans TCF protein, POP-1, converts from repressor to activator as a result of Wnt-induced lowering of nuclear levels. Dev. Biol. *285*, 584–592.

Sternberg, P.W. (2005). Vulval development, In WormBook, The C. elegans Research Community, ed. doi/10.1895/wormbook.1.6.1, http://www.wormbook.org.

Sternberg, P.W., and Horvitz, H.R. (1988). lin-17 mutations of Caenorhabditis elegans disrupt certain asymmetric cell divisions. Dev. Biol. *130*, 67–73.

Strutt, D. (2005). Organ shape: Controlling oriented cell division. Curr. Biol. *15*, R758–R759.

Sulston, J.E., and Horvitz, H.R. (1977). Post-embryonic cell lineages of the nematode, Caenorhabditis elegans. Dev. Biol. *56*, 110–156.

Takeshita, H., and Sawa, H. (2005). Asymmetric cortical and nuclear localizations of WRM-1/beta-catenin during asymmetric cell division in C. elegans. Genes Dev. *19*, 1743–1748.

van de Wetering, M., Cavallo, R., Dooijes, D., van Beest, M., van Es, J., Loureiro, J., Ypma, A., Hursh, D., Jones, T., Bejsovec, A., et al. (1997). Armadillo coactivates transcription driven by the product of the Drosophila segment polarity gene dTCF. Cell *88*, 789–799.

Veeman, M.T., Slusarski, D.C., Kaykas, A., Louie, S.H., and Moon, R.T. (2003). Zebrafish prickle, a modulator of noncanonical Wnt/Fz signaling, regulates gastrulation movements. Curr. Biol. *13*, 680–685.

Wang, Y., and Nathans, J. (2007). Tissue/planar cell polarity in vertebrates: New insights and new questions. Development *134*, 647–658.

Whangbo, J., and Kenyon, C. (1999). A Wnt signaling system that specifies two patterns of cell migration in C. elegans. Mol. Cell *4*, 851–858.

Wodarz, A., and Nathke, I. (2007). Cell polarity in development and cancer. Nat. Cell Biol. *9*, 1016–1024.

Zallen, J.A. (2007). Planar polarity and tissue morphogenesis. Cell *129*, 1051–1063.